Diffusion Restrictions Surrounding Mitochondria: A Mathematical Model of Heart Muscle Fibers

Hena R. Ramay and Marko Vendelin*
Laboratory of Systems Biology, Institute of Cybernetics, Tallinn University of Technology, Tallinn, Estonia

ABSTRACT Several experiments on permeabilized heart muscle fibers suggest the existence of diffusion restrictions grouping mitochondria and surrounding ATPases. The specific causes of these restrictions are not known, but intracellular structures are speculated to act as diffusion barriers. In this work, we assume that diffusion restrictions are induced by sarcoplasmic reticulum (SR), cytoskeleton proteins localized near SR, and crowding of cytosolic proteins. The aim of this work was to test whether such localization of diffusion restrictions would be consistent with the available experimental data and evaluate the extent of the restrictions. For that, a three-dimensional finite-element model was composed with the geometry based on mitochondrial and SR structural organization. Diffusion restrictions induced by SR and cytoskeleton proteins were varied with other model parameters to fit the set of experimental data obtained on permeabilized rat heart muscle fibers. There are many sets of model parameters that were able to reproduce all experiments considered in this work. However, in all the sets, <5–6% of the surface formed by SR and associated cytoskeleton proteins is permeable to metabolites. Such a low level of permeability indicates that the proteins should play a dominant part in formation of the diffusion restrictions.

INTRODUCTION

Intensive structural organization of cardiac myocytes is essential to meet its functional requirements. This alliance starts at micrometer scale where repetitive structural assembly of sarcomeres, invaginations of the sarcolemma (t-tubules), and organelles such as sarcoplasmic reticulum (SR) and mitochondria give rise to macroscopic functionality of the heart, i.e., contraction and relaxation (1). For decades, the electron microscopy has shown that mitochondria are placed along the length of the sarcomere next to the myofilaments and surrounded by a network of thin sarcoplasmic reticulum tubules (2–5). The basic functional association is of energy production (in the form of ATP) by mitochondrion and its utilization by ATPases present in myofilaments and SR. The extent of the tight packing of these organelles, and its effect with regard to their functional association, are still being investigated.

In experiments, the efficiency with which mitochondria produce ATP differs significantly depending on the experimental environment—for example, on whether isolated mitochondria or permeabilized cells are used, or on the location of the source of ADP in cells. When exogenous ADP is supplied to isolated mitochondria, the apparent K_m of respiration is 0.015 mM compared to 0.3 mM in permeabilized myocytes (6,7). This has led to a series of experiments attempting to resolve the discrepancy (8–10). Experimental evidence confirms that in permeabilized fibers, mitochondria are separated from solution by intracellular diffusion restrictions. In such experiments, a compound competing with mitochondria for endogenous ADP was introduced with addition of pyruvate kinase and phosphoenolpyruvate (PK-PEP). In this case, only a 40% decline in respiration rate was seen even with increased concentrations of PK (8,9). However, when trypsin (a protease that disrupts the structural organization of the cells) treated cells were used, a decline of 80% in respiration was observed (9). This suggests the existence of structural restrictions that limit diffusion of substrates inside a cell. A similar conclusion was reached in experiments on contractility of skinned cardiac fibers (10). It was shown that the amount of calcium loaded into SR was dependent on the source of ATP with the endogenous source being considerably more effective than the diffusion of ATP from the surrounding medium. Such cross-talk between ATP consumers and producers in the cell indicates that the cytosol is not a well-mixed environment (11).

In the past, we have developed a series of models to analyze experimental data pointing to the existence of profound diffusion restrictions in cardiac cells. Since skinned cardiac muscle fibers are rather long, diffusion between solution and the intracellular environment should mainly occur in the transversal direction. That is why the first modeling attempts studying the diffusion restrictions were made by using two-dimensional mathematical models describing the diffusion in fiber cross section. In our analysis, we have shown that it is possible to reproduce the preferential access of endogenous ADP to mitochondria as well as the significant increase of apparent K_m(ADP) of mitochondrial respiration in permeabilized fibers by assuming the existence of two

Submitted November 11, 2008, and accepted for publication April 21, 2009.

*Correspondence: markov@ioc.ee

Hena Ramay's present address is Department of Pharmacology and Systems Therapeutics, Mount Sinai School of Medicine, New York, NY.

Editor: Jason M. Haugh.

0006-3495/09/07/0443/10 $2.00

doi: 10.1016/j.bpj.2009.04.062

diffusion restrictions induced by 1), mitochondrial outer membrane; and 2), the intracellular structures limiting diffusion in cytoplasm (12). In that model, we limited diffusion in cytoplasm by reducing apparent diffusion coefficient of ATP and ADP in cytoplasm. According to our simulations (12), it is possible to reproduce relatively small inhibition of respiration by the PK-PEP system if the apparent diffusion coefficient for ATP and ADP is ~20 times smaller than the one measured for skeletal muscle (13). The source of such restriction in the diffusion of ATP and ADP is not clear. To find the possible distribution of diffusion restriction, we composed two models with principally different modes: uniform diffusion restriction and the localized diffusion limitation near mitochondria (14). The analysis revealed that only the second mode, localized diffusion restriction, was able to account for the experimental data. Thus, it was concluded that intracellular diffusion restrictions for adenosine phosphates are not distributed uniformly, but instead, are localized in certain compartments of the cardiac cells (14). Although the previous models give us some insight regarding the processes in the cell, they all used simplified two-dimensional geometry to describe intracellular diffusion (12,14). Thus, it is not clear which intracellular structures could lead to local diffusion restrictions in cardiomyocytes. To study this question, detailed realistic model of intracellular diffusion is needed.

A recent quantitative assessment of mitochondria in the heart using confocal microscopy revealed that they are arranged in a highly ordered crystal-like pattern with relatively constant spacing between adjacent mitochondria (15,16). This regular and distinct placement suggests a spatially localized energy/ATP production role for each mitochondrion as well as promotes intracellular homogeneity of ATP, ADP, inorganic phosphate (P_i), creatine and phosphocreatine. Combined with electron microscopy data showing regularly spaced myofilaments and suggesting that SR is not only found close to mitochondrion but is also seen wrapping around it as thin tubules (2), we hypothesize that SR not only utilizes ATP but may also act as a diffusion barrier leading to functional coupling of ATPases and mitochondria. According to electron microscopy images (3–5), SR forms a netlike structure that can restrict diffusion to a limited extent. However, taking into account tight packing of all proteins in cardiac cells induced by large relative volumes of myofibrils and mitochondria, the neighborhood of SR is occupied by cytoskeleton proteins and other cytosolic proteins. As a result, the environment near SR can be relatively crowded and induce additional diffusion restriction.

The aim of this work is to evaluate whether diffusion restrictions induced by SR and cytoskeleton proteins would be able to explain the available experimental data. For that, a three-dimensional finite element model was constructed and the model solution was compared with the experimental data. The geometry for the mathematical model was composed using the representative structural organization of mitochondrial and SR placement from confocal and electron microscope images. SR and cytoskeleton proteins were assumed to induce diffusion restrictions around mitochondria and in planes between neighboring mitochondria. Those restrictions were varied, as well as a restriction induced by mitochondrial outer membrane, to fit the following set of experimental data: 1), the mitochondrial respiration rate dependence on exogenous ADP and ATP; and 2), the effects of pyruvate kinase and phosphoenolpyruvate additions on respiration.

MATERIALS AND METHODS

Model layout

Our three-dimensional model represents a cross section of the cardiac cells of diameter 10 μm and a thickness of 2 μm with myofibrils distributed evenly in this volume. This thickness of 2 μm represents a single sarcomere that is modeled here as a repetitive structure. In this region, cylindrical mitochondria of radius 0.5 μm and length 2.0 μm were equally spaced at a distance of 1.8 μm as experimentally observed (16). The radius of mitochondria was derived assuming that mitochondria occupy 25% of cell volume.

The diffusion restrictions induced by SR, cytoskeleton proteins, and crowding of cytosolic proteins were localized in the regions of the cell, where SR has been found in electron microscopy studies (2,3,5). In the first arrangement, called MitoR, diffusion restriction was placed around each mitochondrion as a thin cylindrical sheet. In the second arrangement, called BladeR, diffusion restriction was placed as thin rectangular sheets between adjacent mitochondria (see Fig. 1). The ratio of volume of diffusion restrictions to cell volume was kept close to 3%. The diffusion restrictions (MitoR and BladeR) were made permeable by inserting holes into it (Fig. 1, *right*). By variation of the percentage of these holes, the permeability of diffusion restrictions was varied.

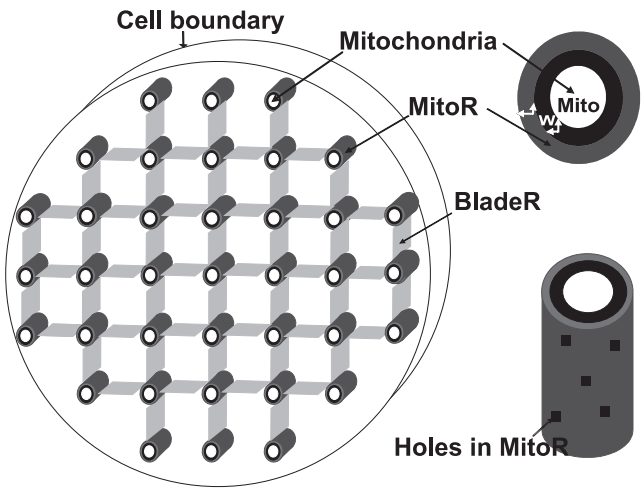

FIGURE 1 Model schema. Representation of a cell cross section with a diameter of 10 μm and a thickness of 2 μm. Mitochondria are placed 1.8-μm apart. There were two diffusion restrictions considered in the work. First, each mitochondrion is surrounded by diffusion restrictions induced by SR, cytoskeleton proteins, and crowding of other proteins in that region (MitoR). In addition, the cell was divided into smaller compartments by bladelike structures representing SR and cytoskeleton proteins (BladeR). Entire surface of diffusion restrictions was partially permeable.

For the sake of simplicity, only two metabolites, ATP and ADP, were included in our reaction scheme. These metabolites were free to diffuse in the cell and the cell membrane was permeable to allow diffusion of these metabolites between the cell and external solution. Since the cell membrane was removed in the experiments by saponin treatment, the permeability of cell surface was set to a very high value leading to the cytosolic concentrations of ATP and ADP near the boundary of the cell equal to the concentrations of the metabolites in solution surrounding the cell. Cytoplasmic ATP was consumed by ATPases (SR and myofibrillar) and regenerated by mitochondria (ATP synthase). Correspondingly, ADP was produced by ATPases and used by mitochondrial ATP synthase. Whereas myofibrillar ATPase was uniformly distributed in cytoplasm, SR ATPase and mitochondrial ATP synthase were modeled as reactions occurring on the boundaries (SR or mitochondria, respectively).

The composed model was used to fit experimental data by varying the following parameters: w, distance between mitochondria and MitoR; P_{MitoR}, part of MitoR surface that is permeable; P_{BladeR}, part of the BladeR surface that is permeable; R_{ATPase}, relative contribution of SR ATPases; K_{ATPase}, apparent K_m(ATP) for all ATPases; and apparent K_m(ADP) for ATP synthesis.

The model details and numerical methods are presented in the Supporting Material.

Experimental data

In this study, we fitted the model parameters by analyzing the set of experimental data used in our earlier studies (12,14).

First, the respiration measurements on permeabilized muscle fibers were reproduced. This was done by finding the apparent K_m of respiration and fitting it to the experimentally determined one: K_m(ADP) of respiration is 0.3 mM with the maximal respiration rate of 14 μmol O_2/(min $\times$ g dw); K_m(ATP) of respiration is 0.2–0.4 mM with the maximal respiration rate of 10 μmol O_2/(min $\times$ g dw). Second, when mitochondrial respiration is stimulated by addition of 2 mM ATP in surrounding solution, it is inhibited by 20–60% after addition of exogenous ATP synthesis (PK+PEP). Third, when mitochondrial respiration is stimulated by injection of 2 mM ATP into ATP and ADP-free medium, the respiration increases relatively fast with the time-constant <60 s.

To convert the total ATP synthase rate to oxygen consumption (VO_2), it was assumed that ATP/O_2 ratio is 6, wet weight to dry weight ratio is 5, and cell volume/wet weight ratio is 0.5 mL/g w/w.

RESULTS

As our previous modeling efforts had pointed toward localized diffusion restrictions, our aim here is to use a more realistic three-dimensional finite element model, as described in Materials and Methods, to test suitability of SR and associated cytoskeleton proteins as the first candidate of diffusion barrier of substrates. The results are presented as follows. We first introduce an example of ADP concentration gradients that are formed due to diffusion intricacies in the model. We then explain the effects of the extent of diffusion barrier around the mitochondria on apparent K_m(ADP) of mitochondrial respiration. After introducing these basic results, we attempt to fit the model by changing the following parameters: 1), w, distance between mitochondria and MitoR; 2), P_{MitoR}, part of MitoR surface that is permeable; 3), P_{BladeR}, part of the BladeR surface that is permeable; 4), R_{ATPase}, relative contribution of SR ATPases; 5), K_{ATPase}, apparent K_m(ATP) for all ATPases; and 6), apparent K_m(ADP) for ATP synthesis ($K_{ATPsyn,m}$ in Eq. S12 in the Supporting Material).

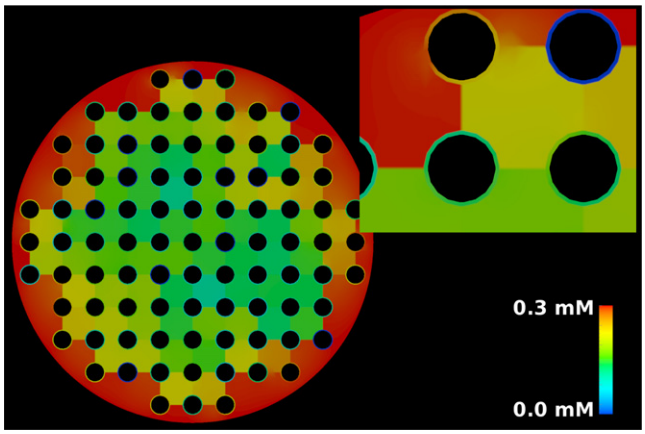

FIGURE 2 ADP gradients in the model after 0.3 mM of ADP was added to the solution and steady state was achieved (magnified view in *inset*). In these simulations, ADP was kept at 0.3 mM in solution and stimulated respiration of mitochondria inside the cells. Note that the steep gradients are formed next to mitochondria and between mitochondria, where diffusion was hindered by barriers.

ADP gradients in the model

To illustrate how the introduced localized diffusion barriers act, in Fig. 2, we show [ADP] concentrations at steady state after addition of 0.3 mM of ADP to the external solution. For the parameter values used in this simulation, ADP diffusion from the cell boundary forms gradients for three reasons. First, because the cell interior itself is not fully permeable to ADP and a concentration gradient is induced by diffusion in the cytoplasm. Second, the BladeR and MitoR that are placed over the grid are impermeable to substrates, hence ADP diffuses through the narrow opening between the diffusion restrictions and through the opening within the MitoR and BladeR. Third, very localized gradients occur between the mitochondria and MitoR region due to ATP synthase activity and relatively small permeability of MitoR (Fig. 2, *inset*).

Permeability of SR/cytoskeleton proteins and changes in K_m(ADP) of mitochondrial respiration

An example of how changes in permeability of the MitoR (when placed at different distances from mitochondria) affect apparent K_m(ADP) of mitochondrial respiration is shown in Fig. 3. As the fraction of the open surface of MitoR decreases, the diffusion restriction between mitochondria and the rest of the cell increases. As a result, one has to add more ADP into solution to reach the same respiration rate. Thus, apparent K_m(ADP) of mitochondrial respiration increases with the reduction of open surface of MitoR. This general principle holds for all distances (w) between the mitochondria and MitoR. However, variation of w leads

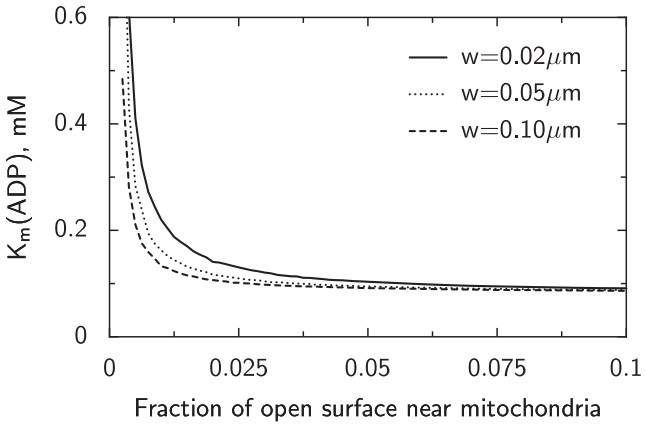

FIGURE 3 Apparent K_m(ADP) of oxidative respiration depends on the diffusion restrictions between solution surrounding fiber and mitochondria. Here, it is demonstrated that K_m(ADP) decreases with increasing MitoR cylinder permeability. Note that the distance between mitochondria and MitoR cylinder plays a role as well (distance was given by parameter w).

to changes in apparent K_m(ADP) dependency on the permeability of MitoR. Namely, as the distance between the mitochondria and MitoR decreases, the K_m(ADP) dependency shifts to the right (Fig. 3). This is induced by limited space between MitoR and mitochondria. In all of these plots, K_m(ADP) forms an exponential relationship with permeability of the MitoR surface, where >2% of open surface results in K_m(ADP) of <0.2 mM. When the open surface is kept <2%, we noticed that a wide range of model parameters could reproduce realistic K_m values. Such a low permeability suggests that SR is not the main diffusion barrier, and that the diffusion has to be restricted mostly by cytoskeleton and other proteins grouped together in the cell regions.

Parameter range for successful simulations

The model has a large set of parameters. As a result, there can be more than one set of parameters able to reproduce the experimental data. To find such parameter value sets, we varied the model parameters and compared the model solution with the following experimental data: apparent K_m(ADP) of respiration is 0.3 mM, apparent K_m(ATP) of respiration is 0.2–0.4 mM, inhibition of respiration by exogenous ATP synthesis (PK+PEP) is 20–60%, and time-constant after ATP addition is <60 s. The varied model parameters and the ranges were: w, distance between mitochondria and MitoR (0.01–0.1 μm); P_{BladeR}, part of the BladeR surface that is permeable (0.5–10%); R_{ATPase}, relative contribution of SR ATPases (5–95%); K_{ATPase}, apparent K_m(ATP) for all ATPases (0.05–0.3 mM); and apparent K_m(ADP) for ATP synthesis (0.025–0.25 mM). To find P_{MitoR} corresponding to each selected set, we used the monotonic relationship between apparent K_m(ADP) of mitochondrial respiration and P_{MitoR} (Fig. 3). Namely, we found P_{MitoR} by fitting the computed apparent K_m(ADP) of mitochondrial respiration to the assumed experimental value of 0.3 mM. Since the relationship between P_{MitoR} and apparent K_m(ADP) depended on other model parameters, this procedure had to be repeated for each considered set of parameters. Note that, sometimes, apparent K_m(ADP) was too high even with the completely open MitoR. This could occur if other diffusion restrictions were too high. In such cases, the set of parameters was considered as not corresponding to the experimental data and all further simulations with this set were omitted. A simulation with a particular set of model parameters was regarded successful if all four of the experimental constraints were matched. We checked a total of 10,584 model parameter combinations, out of which 1413 were successful.

Fig. 4 shows results for all parameters in the successful simulations range. These results demonstrate that many combinations of these parameters can follow our four constraints. From these simulations we are also able to make deductions about ranges of free parameters for which the constraints were met. These ranges are determined (within the simulated ranges) by the fact that for some parameters, the number of successful simulations increases to a maximum value and then slowly decreases back to almost 0. The ranges for P_{MitoR} and P_{BladeR} reflect a very low permeability through studied diffusion restrictions. Less than 8% of these surfaces are open for diffusion of substrates. The apparent K_m(ADP) of mitochondrial ATP synthase is <0.2 mM for our model parameters, suggesting that the diffusion restriction induced by the mitochondrial outer membrane is moderate. Note that while the range of several parameters can be estimated from the simulations, relative contribution of SR ATPases and the distance between mitochondria and surrounding SR cannot be determined based on the experiments used.

Although we can determine the range of some parameter values, it should be noted that the ranges of the model parameters are not independent from each other. This is illustrated in Fig. 5, where the count of successful simulations as a function of two model parameters is shown by color maps. These maps clearly display how the parameters influence the optimal values of each other by shifting the range of parameter values with the largest number of successful simulations. Thus, if one or more parameters would be determined experimentally, the range of other parameter values that are able to reproduce the experiments analyzed here could be refined.

We could use the found range of successful simulations to predict the apparent intracellular K_m(ADP) of respiration. For that, we found the mean ADP concentration in the fiber when respiration was stimulated by exogenous 0.3 mM ADP, i.e., apparent K_m(ADP) of respiration for exogeneous ADP. The simulations were performed for all successful sets of model parameters with the distribution function describing the mean ADP concentration shown in Fig. 6. As it is clear from our results, the mean ADP concentration depends on the model parameters with the variation of mean ADP concentration 0.15–0.275 mM.

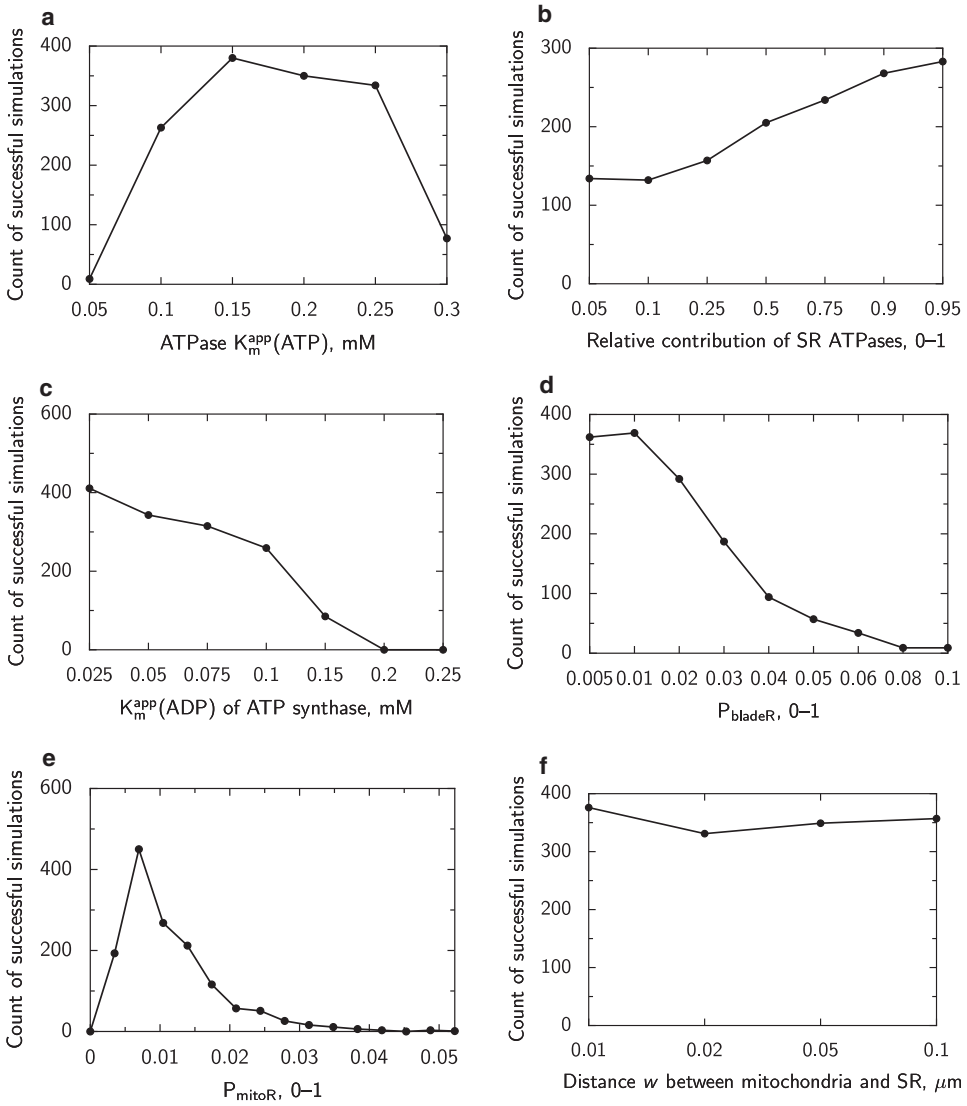

FIGURE 4 Number of simulations that reproduced the experimental set for each of the parameters. In the figure, apparent K_m constants for ATPase and ATPsynthase correspond to K_{ATPase} and $K_{ATPsyn,m}$ in Eq. S11 and Eq. S12. Note that for some parameters, the simulations were able to reproduce the experimental data only in the certain range of values. Thus, it is possible to determine from simulations the range of ATPase K_m(ATP), ATP synthase K_m(ADP), and permeability of diffusion barriers. However, relative contribution of ATPases and the distance between mitochondria and SR cannot be determined based on simulated experiments.

DISCUSSION

The model presented in this work was designed to analyze intracellular diffusion occurring in permeabilized rat cardiac muscle fiber. With this detailed three-dimensional model, we have looked at structural organization of the mitochondria, SR, and cytoskeleton proteins to analyze the influence of intracellular environment on the mitochondrial function. To our knowledge, this model is the first three-dimensional model with realistic structural details to study intracellular diffusion restrictions. A series of models by our group have been presented in the past (12,14). Those models have been essential for settling the experimental discrepancy of apparent K_m(ADP) for respiration in isolated and in situ mitochondria by pinpointing that local diffusion restrictions exist. However, these models had simplified two-dimensional geometry to describe intracellular diffusion. Thus, it was not clear from these models which of the structures could lead to local diffusion restrictions. To this end, our three-dimensional model is an improvement with realistic structural details and a thorough analysis of wide parameter ranges.

The main finding of this work is that the studied diffusion restrictions (MitoR and BladeR) may form barricades with very low permeability for metabolites. We have tested the hypothesis according to which the diffusion restrictions in cardiomyocytes are induced by SR and associated cytoskeleton proteins. According to our simulations, this hypothesis does not contradict the experimental data against which it was tested. Based on the hypothesis, we predict very low permeability of SR and associated cytoskeleton proteins. Taking into account that SR forms a loose network with large openings in it, such low permeability clearly indicates that the diffusion restrictions modeled by BladeR and MitoR are mainly imposed by cytoskeleton as well as crowding of other proteins in that part of the cell.

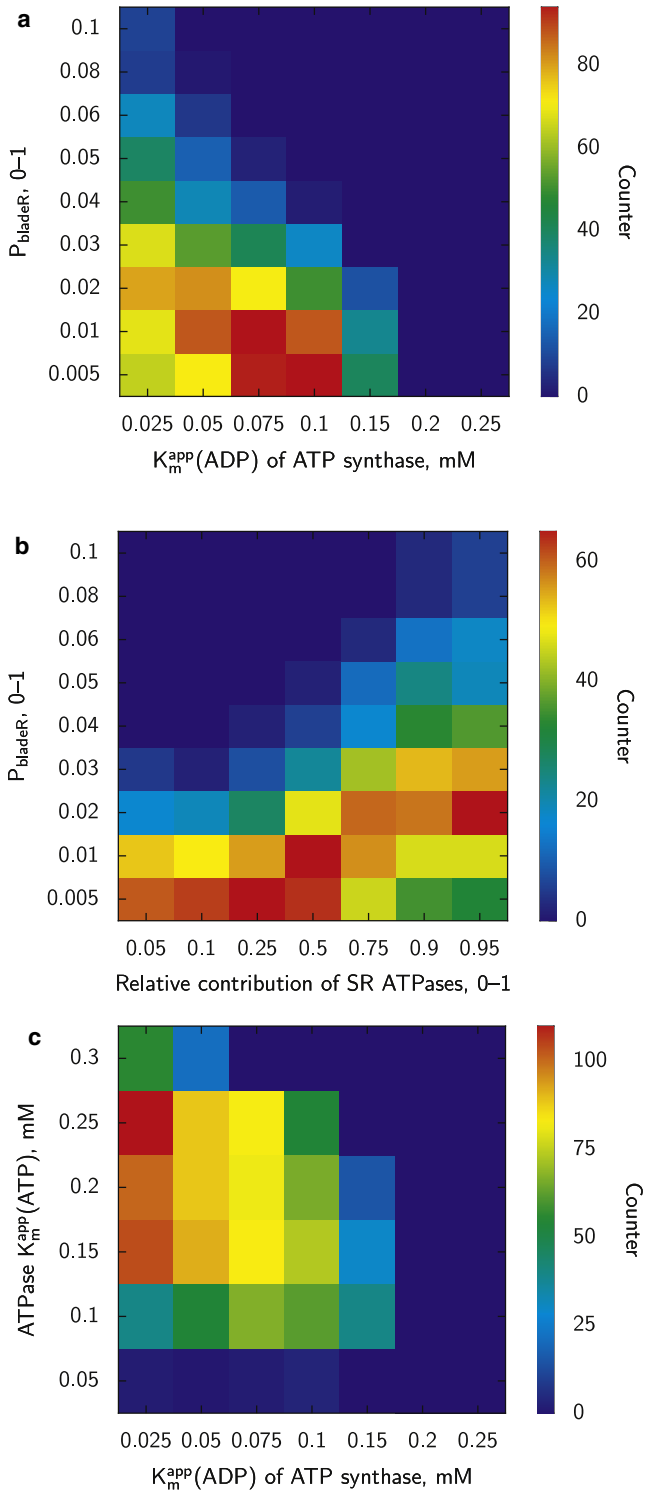

FIGURE 5 Distribution of parameter values able to reproduce the experimental data. In the figure, apparent K_m constants for ATPase and ATPsynthase correspond to K_{ATPase} and $K_{ATPsyn,m}$ in Eq. S11 and Eq. S12. Note that the parameter values that are able to reproduce experimental data depend on the values of other parameters.

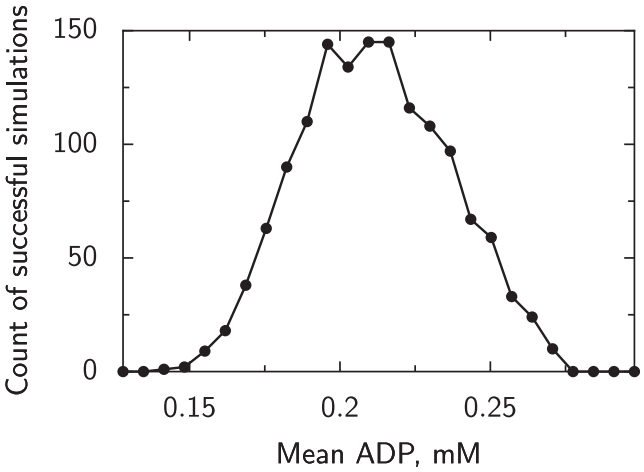

FIGURE 6 Mean concentration of ADP in the fiber during stimulation of respiration by exogenous 0.3 mM ADP. The mean ADP concentration was calculated for all successful parameter sets and is presented here as a distribution function. Note that the mean ADP concentration of ~0.21 mM was recorded for the largest number of tested successful parameter sets.

Model assumptions

The main assumption of the model is the existence of localized diffusion restrictions in cardiomyocytes and positioning of those restrictions in the location occupied by SR and associated cytoskeleton proteins. This assumption is based on the following.

First, as mentioned in the Introduction, the cross-talk between mitochondria and intracellular ATPases recorded in several experiments (8–10) indicates the existence of diffusion restrictions (11,12). Indeed, without diffusion restrictions grouping ATPases and mitochondria together in permeabilized cardiac muscle fiber preparation, oxygen respiration would be completely inhibited by a competitive ATP-regeneration system (8,9) and loading of sarcoplasmic reticulum by calcium would not depend on mitochondrial respiration (10).

Second, according to our analysis (14), the diffusion restrictions in cardiomyocytes are not distributed uniformly, but instead are localized in certain areas. Given the assumptions of our models, it is impossible to fit several of the experiments performed on permeabilized cardiac muscle fibers if the diffusion is restricted uniformly in myoplasm and myofibrils (14). On the other hand, when diffusion restrictions were localized in certain areas of the cell, the model was able to fit all the tested measurements (14). Although the fit was not perfect and there were two parameter sets required to reproduce all the data with the model that assumed localized diffusion restrictions, no sets were found that reproduced the measured data when the uniform diffusion restriction was assumed. Thus, the localized diffusion restriction distribution was used as a basis in this study.

Third, the region in cardiac cell that would possibly restrict diffusion in localized manner is between myofibrils

and next to mitochondria. According to electron microscopy studies of the cardiac muscle cells, those are positions where SR membranes are localized (2,3). Such localized diffusion restrictions are not expected in the myofibrils where actin and myosin form a highly packed environment, since that part of the muscle cell would probably restrict diffusion rather uniformly.

Geometry of the model was composed by taking advantage of the differences in dimensions of the fiber. The fibers are rather long compared to their diameter. Thus, after permeabilization, one can assume that the diffusion restrictions detected in the experiments are induced for the movement of molecules in transversal direction. Taking this into account, we took one repetitive unit—a sarcomere—and modeled three-dimensional diffusion within the cross section of the fiber that is one-sarcomere-length long. The diameter of the fiber was taken to be equal to the diameter of a cardiac cell, ~20 μm. This was based on the fact that the apparent K_m(ADP) of respiration is the same for permeabilized cardiomyocytes and muscle fibers (17), indicating the similar overall diffusion restriction between mitochondria and surrounding solution. In the model, we positioned mitochondria on the square lattice with the 1.8-μm distance between mitochondrial centers. The hexagonal packing would be closer to the distribution of mitochondria relative to each other, as determined from the analysis of confocal images (16). However, generation of finite element mesh using the square lattice was not trivial and we limited this study with that geometry for simplicity.

In addition to simplification of geometry, we used a simple Michaelis-Menten type equation to model oxidative phosphorylation. Namely, ATP synthesis activity by mitochondria was determined by the maximal rate and apparent K_m(ADP). Thus, we ignore the regulatory role of P_i, which is expected to be high in vivo based on analysis of mathematical models and experimental data (18,19). However, in analyzed experiments, the level of control of P_i is expected to be similar for all mitochondria in the cell. Namely, P_i concentration was 3 mM and, assuming the same diffusion restrictions for P_i as for ATP and ADP, we would expect the gradient to be only ~10% in the case of apparent K_m(ADP) measurements. At this concentration range, 10% variation is not expected to influence mitochondrial respiration significantly. Additionally, due to the strong buffering, the calcium regulatory role was also expected to be homogeneous in the cell.

Predictions

Based on our simulation results, we predict that the SR and associated structures form diffusion restrictions with very low permeability for metabolites. Since the diffusion restrictions were induced by considering SR and associated proteins as an obstacle in the way of the metabolites in the model, the diffusion of all molecules in the cell is predicted to be constrained via a similar mechanism. In the regions of the cardiac muscle cells occupied by SR and associated cytoskeleton proteins, <5–6% of the surface is permeable to metabolites. This indicates a very high level of packing between myofibrils and around mitochondria. According to our simulations, it is possible that the degree in packing of impermeable structures is somewhat different in those regions of the cell. This is indicated by the different distribution of successful simulations as functions of permeability of diffusion restrictions between myofibrils P_{BladeR} and surrounding mitochondria P_{MitoR} (Fig. 4). However, for both diffusion restrictions, the small part of the surface that is permeable indicates that the cytoskeleton proteins should play a dominant part in formation of the restrictions.

In our model, we distinguished diffusion restriction induced by mitochondrial outer membrane from diffusion restriction formed by SR and associated cytoskeleton proteins. In interpreting the modeling results, we assume that the differences in mitochondrial oxidative phosphorylation between isolated mitochondria and mitochondria in permeabilized fibers are only induced by the differences in mitochondrial outer membrane permeability. It is assumed that the membrane is highly permeable in isolated mitochondria and that the permeability can be lower in permeabilized fiber preparation. Thus we assume that saponin treatment of the fibers does not influence intramitochondrial oxidative phosphorylation significantly. The diffusion restriction induced by mitochondrial outer membrane was modeled by changing the apparent K_m(ADP) of ATP synthase. In this notation, the larger diffusion restriction would lead to the larger value of K_m(ADP). Since the apparent K_m(ADP) of isolated mitochondria is close to 0.015–0.020 mM, any increase over that value would indicate existence of diffusion restriction on the mitochondrial outer membrane level. According to our analysis, the model was able to reproduce the experimental data only when K_m(ADP) was <0.2 mM (Fig. 4). There are few model combinations that are consistent with the experimental data at K_m(ADP) value of 0.15 mM, with the largest number of combinations at lower values of K_m(ADP) ($\leq$0.1 mM). From this, we conclude that diffusion restrictions induced by mitochondrial outer membrane are probably moderate. Note that the largest possible diffusion restriction on mitochondrial outer membrane predicted by our model (K_m(ADP) = 0.15 mM) would suggest a very small permeability of diffusion restrictions between myofibrils P_{BladeR}. This becomes clear from dependence of the number of successful simulations on K_m(ADP) and P_{BladeR} (Fig. 5 *A*).

To get an estimation of the extent of diffusion restriction induced by mitochondrial outer membrane, isolated mitochondria preparation can be used with the gradual reconstruction of intracellular medium. Such measurements were performed on isolated brain mitochondria (20). After incubation with tubulin, it is possible to analyze the respiration of isolated mitochondria, assuming the existence of two subpopulations. Whereas one of those subpopulations had

an apparent K_m(ADP) that would be expected for isolated mitochondria (0.007 ± 0.002 mM), the second population of isolated mitochondria had a high apparent K_m(ADP) equal to 0.17 ± 0.05 mM. Such high apparent K_m(ADP) for isolated mitochondria is probably induced by interaction between tubulin and the voltage-dependent anion channel on the outer membrane of mitochondria. Whether interaction between tubulin and the voltage-dependent anion channel would lead to apparent K_m(ADP) that is so high in permeabilized cardiac muscle cell is not known and requires further investigation. According to our analysis, it would then be on the border range of the values predicted by our model (K_m(ADP) of ATP synthase $\leq$0.15 mM) and would suggest a very high level of diffusion restrictions induced by SR and cytoskeleton proteins between myofibrils (BladeR, Fig. 5 *A*).

The combination of mitochondrial outer membrane and MitoR restriction would determine the diffusion restriction between mitochondrial oxidative phosphorylation and actomyosin ATPases. One way to access the extent of such diffusion restriction is to find mean ADP concentration in the fiber during stimulation of respiration by exogeneous ADP. At exogeneous 0.3 mM ADP (apparent K_m(ADP) in permeabilized fibers), mean intracellular ADP concentration was found to be between 0.15 and 0.275 mM, depending on the used model parameter set (Fig. 6). Those values are considerably higher than apparent K_m(ADP) of oxidative phosphorylation of isolated mitochondria indicating the profound role of MitoR and mitochondrial outer membrane in regulation of oxidative phosphorylation in vivo.

We modeled ATPase activity by assuming that the ATPases associated with SR and myofibrils have the same apparent K_m(ATP). Such simplification was made to reduce the number of model parameters. K_m(ATP) was varied from 0.05 mM to 0.3 mM and the model was able to find the sets of parameters that were consistent with the analyzed experimental data only if apparent ATPase K_m(ATP) was $\geq$0.1 mM. As it is clear from our analysis, the most probable value of apparent K_m(ATP) of ATPases is between 0.1 and 0.25 mM (Fig. 4 and Fig. 5 *C*).

There were two model parameters that we were not able to determine from our simulations: relative contribution of SR ATPases (R_{ATPase}), and the distance between mitochondria and surrounding SR (w). For both of these parameters, the number of successful model combinations stayed relatively large, regardless of the selected parameter value (Fig. 4 and Fig. 5 *B*). Thus, to determine the relative contribution of SR and myofibrillar ATPases in relaxed skinned cardiac muscle fiber preparation as well as the distance between mitochondria and surrounding SR, additional experiments have to be performed and analyzed.

Physiological implications

Recently we have demonstrated that the diffusion of fluorescently labeled ATP (Alexa-ATP) is anisotropic in rat cardiomyocytes (21). When measured using raster image correlation spectroscopy (RICS), the average diffusion coefficient of Alexa-ATP in longitudinal direction is ~2 times smaller than in solution surrounding the cells. The reduction of the diffusion coefficient in transversal direction was more profound—~3.5 times smaller value was obtained than in solution. The source of such anisotropy is not clear, but it can be attributed to the anisotropic arrangement of diffusion obstacles such as mitochondria, SR, and myofibrils in cardiomyocytes (21). The low permeability of diffusion barriers induced by SR, and associated cytoskeleton proteins suggested by the results of our analysis, is consistent with the anisotropy of the average diffusion coefficient due to the arrangement of those barriers. Although the reduction of diffusion coefficient estimated by RICS was not as profound as the estimation found in our simulations, the differences can be attributed to the nature of diffusion restrictions. Namely, in RICS, the correlation between fluctuations in the acquired images is averaged over the studied region, leading to the estimation of mean diffusion coefficient in that region. As a result of such averaging, we expect that the diffusion restrictions that are not distributed over a larger spatial region would not influence the correlation functions too much and, as a result, would lead only to smaller modulation in the estimation of the diffusion coefficients.

The low permeability of SR and associated cytoskeleton proteins is consistent with the analysis of ATP and phosphocreatine by ^{31}P-NMR diffusion spectroscopy measurements in muscle fibers of lobster (22) and in rat skeletal muscle (23). According to that analysis, diffusion of metabolites was restricted by cylindrically shaped restrictions that had a diameter several times smaller than the studied cells. It was suggested that those restrictions could be induced by SR (22), in agreement with our results.

The physiological role of diffusion restrictions between myofibrils and surrounding mitochondria is not yet clear. The existence of strong diffusion barriers near mitochondria may provide mechanistic explanation to transients in mitochondrial calcium levels observed in cardiomyocytes. Indeed, although the close contacts between endoplasmic reticulum and mitochondria has been known for a while (24), the distance between calcium release units and mitochondria is considered to be relatively large and there is a small chance of direct molecular link between calcium release units and mitochondria (25,26). The diffusion restrictions induced by cytoskeleton proteins, for example, may facilitate formation of calcium microdomains that could explain calcium transients in mitochondrial matrix. Formation of intracellular clusters of oscillating mitochondria in substrate deprivation conditions (27) is also consistent with the diffusion barriers. The oscillation of mitochondrial bioenergetic state as measured by fluorescence of endogenous flavoprotein and mitochondrial membrane potential sensitive dyes, can be either on the whole cell range or in a subcellular region (27,28). With the reactive oxygen

species suggested as a signal synchronizing mitochondrial oscillations and leading to the waves of mitochondrial redox states (28–30), diffusion restrictions between myofibrils can provide barriers that would lead to the sharp borders between oscillating and nonoscillating regions of the cell as reported in Romashko et al. (27).

Although high level of organization of intracellular structures is common for healthy rat cardiomyocytes, strong changes in organization occur in pathological conditions. It has been shown that such changes in structure are correlated with changes in overall diffusion restrictions as measured by apparent K_m(ADP) of mitochondrial respiration in skinned fibers (31). Recently, it has been suggested that the structural changes after heart failure reduce the intimate links between mitochondria and surrounding ATPases (32). This conclusion was based on the comparison of interaction between mitochondria and myofibrillar actomyosin ATPase in the fibers isolated from control or heart-failure rats. Based on our results, we predict that the changes in intracellular organization would lead to changes in diffusion restrictions imposed by SR and associated cytoskeleton proteins. What the role of diffusion restrictions in formation of intracellular energy fluxes may be, and how those fluxes are altered in pathological conditions, is a subject for further study.

In conclusion, we have shown that the analyzed measurements can be reproduced, assuming that the diffusion restrictions in rat cardiac muscle fibers are induced by SR and associated cytoskeleton proteins. Although the presented results do not prove that the intracellular diffusion restrictions are distributed as assumed here, we have made several predictions that can be tested against experimental data. Based on our analysis, we predict very low permeability of SR and associated cytoskeleton proteins. Such a low permeability of diffusion restrictions indicates that the restrictions are mainly imposed by cytoskeleton proteins and the crowding of other proteins.

SUPPORTING MATERIAL

One table and 14 equations are available at http://www.biophysj.org/biophysj/supplemental/S0006-3495(09)00979-5.

We thank Dr. Rikke Birkedal (Institute of Cybernetics at Tallinn University of Technology, Estonia) for interesting discussions.

This work was supported by the Wellcome Trust (Fellowship No. WT081755MA) and European Union Marie Curie Host Fellowship for the Transfer of Knowledge (grant No. MTKD-CT-2004-013909 to H.R.).

REFERENCES

1. Bers, D. 2002. Cardiac excitation-contraction coupling. *Nature*. 415:198–205.
2. Lukyanenko, V., A. Ziman, A. Lukyanenko, V. Salnikov, and W. J. Lederer. 2007. Functional groups of ryanodine receptors in rat ventricular cells. *J. Physiol.* 583:251–269.
3. Segretain, D., A. Rambourg, and Y. Clermont. 1981. Three-dimensional arrangement of mitochondria and endoplasmic reticulum in the heart muscle fiber of the rat. *Anat. Rec.* 200:139–151.
4. Ogata, T., and Y. Yamasaki. 1990. High-resolution scanning electron microscopic studies on the three-dimensional structure of the transverse-axial tubular system, sarcoplasmic reticulum and intercalated disc of the rat myocardium. *Anat. Rec.* 228:277–287.
5. Territo, P. R., S. A. French, M. C. Dunleavy, F. J. Evans, and R. S. Balaban. 2001. Calcium activation of heart mitochondrial oxidative phosphorylation: rapid kinetics of MVO_2, NADH, and light scattering. *J. Biol. Chem.* 276:2586–2599.
6. Kümmel, L. 1988. Ca,Mg-ATPase activity of permeabilized rat heart cells and its functional coupling to oxidative phosphorylation of the cells. *Cardiovasc. Res.* 22:359–367.
7. Saks, V. A., Y. O. Belikova, and A. V. Kuznetsov. 1991. In vivo regulation of mitochondrial respiration in cardiomyocytes: specific restrictions for intracellular diffusion of ADP. *Biochim. Biophys. Acta.* 1074:302–311.
8. Seppet, E. K., T. Kaambre, P. Sikk, T. Tiivel, H. Vija, et al. 2001. Functional complexes of mitochondria with Ca,Mg-ATPases of myofibrils and sarcoplasmic reticulum in muscle cells. *Biochim. Biophys. Acta.* 1504:379–395.
9. Saks, V. A., T. Kaambre, P. Sikk, M. Eimre, E. Orlova, et al. 2001. Intracellular energetic units in red muscle cells. *Biochem. J.* 356:643–657.
10. Kaasik, A., V. Veksler, E. Boehm, M. Novotova, A. Minajeva, et al. 2001. Energetic crosstalk between organelles: architectural integration of energy production and utilization. *Circ. Res.* 89:153–159.
11. Weiss, J. N., and P. Korge. 2001. The cytoplasm: no longer a well-mixed bag. *Circ. Res.* 89:108–110.
12. Saks, V., A. Kuznetsov, T. Andrienko, Y. Usson, F. Appaix, et al. 2003. Heterogeneity of ADP diffusion and regulation of respiration in cardiac cells. *Biophys. J.* 84:3436–3456.
13. Kushmerick, M. J., and R. J. Podolsky. 1969. Ionic mobility in muscle cells. *Science.* 166:1297–1298.
14. Vendelin, M., M. Eimre, E. Seppet, N. Peet, T. Andrienko, et al. 2004. Intracellular diffusion of adenosine phosphates is locally restricted in cardiac muscle. *Mol. Cell. Biochem.* 256/257:229–241.
15. Vendelin, M., N. Beraud, K. Guerrero, T. Andrienko, A. Kuznetsov, et al. 2005. Mitochondrial regular arrangement in muscle cells: a ''crystal-like'' pattern. *Am. J. Physiol. Cell Physiol.* 288:C757–C767.
16. Birkedal, R., H. A. Shiels, and M. Vendelin. 2006. Three-dimensional mitochondrial arrangement in ventricular myocytes: from chaos to order. *Am. J. Physiol. Cell Physiol.* 291:C1148–C1158.
17. Saks, V. A., V. I. Veksler, A. V. Kuznetsov, L. Kay, P. Sikk, et al. 1998. Permeabilized cell and skinned fiber techniques in studies of mitochondrial function in vivo. *Mol. Cell. Biochem.* 184:81–100.
18. Saks, V. A., O. Kongas, M. Vendelin, and L. Kay. 2000. Role of the creatine/phosphocreatine system in the regulation of mitochondrial respiration. *Acta Physiol. Scand.* 168:635–641.
19. Bose, S., S. French, F. J. Evans, F. Joubert, and R. S. Balaban. 2003. Metabolic network control of oxidative phosphorylation: multiple roles of inorganic phosphate. *J. Biol. Chem.* 278:39155–39165.
20. Monge, C., N. Beraud, A. V. Kuznetsov, T. Rostovtseva, D. Sackett, et al. 2008. Regulation of respiration in brain mitochondria and synaptosomes: restrictions of ADP diffusion in situ, roles of tubulin, and mitochondrial creatine kinase. *Mol. Cell. Biochem.* 318:147–165.
21. Vendelin, M., and R. Birkedal. 2008. Anisotropic diffusion of fluorescently labeled ATP in rat cardiomyocytes determined by raster image correlation spectroscopy. *Am. J. Physiol. Cell Physiol.* 295:C1302–C1315.
22. Kinsey, S. T., and T. S. Moerland. 2002. Metabolite diffusion in giant muscle fibers of the spiny lobster *Panulirus argus*. *J. Exp. Biol.* 205: 3377–3386.
23. de Graaf, R. A., A. van Kranenburg, and K. Nicolay. 2000. In vivo ^{31}P-NMR diffusion spectroscopy of ATP and phosphocreatine in rat skeletal muscle. *Biophys. J.* 78:1657–1664.
24. Rizzuto, R., P. Pinton, W. Carrington, F. S. Fay, K. E. Fogarty, et al. 1998. Close contacts with the endoplasmic reticulum as determinants of mitochondrial Ca^{2+} responses. *Science.* 280:1763–1766.

25. Sharma, V. K., V. Ramesh, C. Franzini-Armstrong, and S. S. Sheu. 2000. Transport of Ca^{2+} from sarcoplasmic reticulum to mitochondria in rat ventricular myocytes. *J. Bioenerg. Biomembr.* 32:97–104.

26. Franzini-Armstrong, C. 2007. ER-mitochondria communication. How privileged? *Physiology (Bethesda).* 22:261–268.

27. Romashko, D. N., E. Marban, and B. O'Rourke. 1998. Subcellular metabolic transients and mitochondrial redox waves in heart cells. *Proc. Natl. Acad. Sci. USA.* 95:1618–1623.

28. Aon, M. A., S. Cortassa, E. Marban, and B. O'Rourke. 2003. Synchronized whole cell oscillations in mitochondrial metabolism triggered by a local release of reactive oxygen species in cardiac myocytes. *J. Biol. Chem.* 278:44735–44744.

29. Cortassa, S., M. A. Aon, R. L. Winslow, and B. O'Rourke. 2004. A mitochondrial oscillator dependent on reactive oxygen species. *Biophys. J.* 87:2060–2073.

30. Brady, N. R., S. P. Elmore, J. J. H. G. M. van Beek, K. Krab, P. J. Courtoy, et al. 2004. Coordinated behavior of mitochondria in both space and time: a reactive oxygen species-activated wave of mitochondrial depolarization. *Biophys. J.* 87:2022–2034.

31. Boudina, S., M. N. Laclau, L. Tariosse, D. Daret, G. Gouverneur, et al. 2002. Alteration of mitochondrial function in a model of chronic ischemia in vivo in rat heart. *Am. J. Physiol. Heart Circ. Physiol.* 282:H821–H831.

32. Joubert, F., J. R. Wilding, D. Fortin, V. Domergue-Dupont, M. Novotova, et al. 2008. Local energetic regulation of sarcoplasmic and myosin ATPase is differently impaired in rats with heart failure. *J. Physiol.* 586:5181–5192.